Electronic Supplementary Material (ESI) for ChemComm.

Supporting information for

Composition space of PtIrPdRhRu high entropy alloy nanoparticles synthesized by solvothermal reactions

Andreas Dueholm Bertelsen, Alexander Reinhardt Hansen, Nils Lau Nyborg Broge, Aref Mamakhel, Bo Brummerstedt Iversen*

Center for Integrated Materials Research, Department of Chemistry and iNANO, Aarhus University, DK-8000 Aarhus C, Denmark

*Corresponding author: bo@chem.au.dk

Table of Content

Nomenclature

For convenience a description of the nomenclature of samples is repeated. Each series of samples varies the concentration from equimolar to purely one PGM with intermediate steps of 40, 60, 80, and 96 at% exemplified here by the platinum series: Pt0.2Ir0.2Pd0.2Rh0.2Ru0.2, Pt0.4(IrPdRhRu)0.6, Pt0.6(IrPdRhRu)0.4, Pt0.8(IrPdRhRu)0.2, Pt0.96(IrPdRhRu)0.04 and Pt. The samples will be referred to by their main PGM and the at% of the PGM, thus listed above will be equimolar, Pt0.4, Pt0.6, Pt0.8, Pt0.96, and Pt respectively.

Experimental

Chemicals

The metal precursors Ir(acac)$_3$ 97%, Rh(acac)$_3$ 97%, and Pd(acac)$_2$ 99% were purchased from Sigma–Aldrich. Pt(acac)$_2$ ≥48% (metal based) was purchased from Alfa Aesar and Ru(acac)$_3$ 26.13% (metal basis) from Chempur. HPLC grade acetone and abs. ethanol were from VWR.

Synthesis

Solutions of each precursor with a total metal concentration of 10 mM were prepared by dissolving the relevant amounts of reactants in a 50:50 vol% mixture of HPLC grade acetone and abs. ethanol. The precursors with Ru and Pt were shaken for 5 minutes to properly dissolve the initial solution. The precursors with Pd, Rh, and Ir were stirred for one hour as they were harder to dissolve. The precursor solutions were made in batches of 100 mL except for Pd which was made as a 20 mL precursor solution before each synthesis due to the instability of dissolved palladium over time. A total of 10 mL precursor solution was prepared in appropriate concentrations from the batch solutions. This was added to a 20 mL Teflon-lined steel autoclave and placed in a 200 °C preheated oven for 24 hours. Upon removal, the autoclaves were cooled passively to ambient temperature. The collected powders were washed with acetone twice.

Characterization

All Powder X-ray diffraction (PXRD) data were collected on a Rigaku Smartlab diffractometer with a Cu Kα_1 source. The samples were deposited on a flat Si(111) surface by drop-casting a suspension of the synthesized particles. The data were measured in Bragg-Brentano geometry. The suspensions were prepared by mixing powders and acetone and ultrasonicated for at least 30 minutes.

This sample preparation for PXRD (drop casting) results in a variation in the illuminated volume with scattering angle and a Le Bail fit was performed to extract the unit cell parameters. A cosine shift correction for imperfect sample position was employed. The background was modelled using a 3rd

order Chebyshev polynomial. The modified Thompson-Cox-Hastings pseudo-Voigt was used as peak shape model with parameters X and Y as refined parameters.

High-resolution electron microscopy images were measured on a FEI "Talos" F200X analytical (S)TEM-microscope both in TEM and STEM mode. The samples were dropped on 3 mm circular Cu/C grids. A single drop of ethanol dispersed sample was added to each disc for analysis. The machine was operated at 200keV, and a 4k x 4k Ceta 16M camera was used for bright field images. Energy-dispersive spectroscopy (EDS) was measured with a ChemiSTEM X-ray detection system while dark field images were acquired on a HAADF imaging detector with collection angle 60-200 mrad.

Additional PXRD and TEM of selected samples

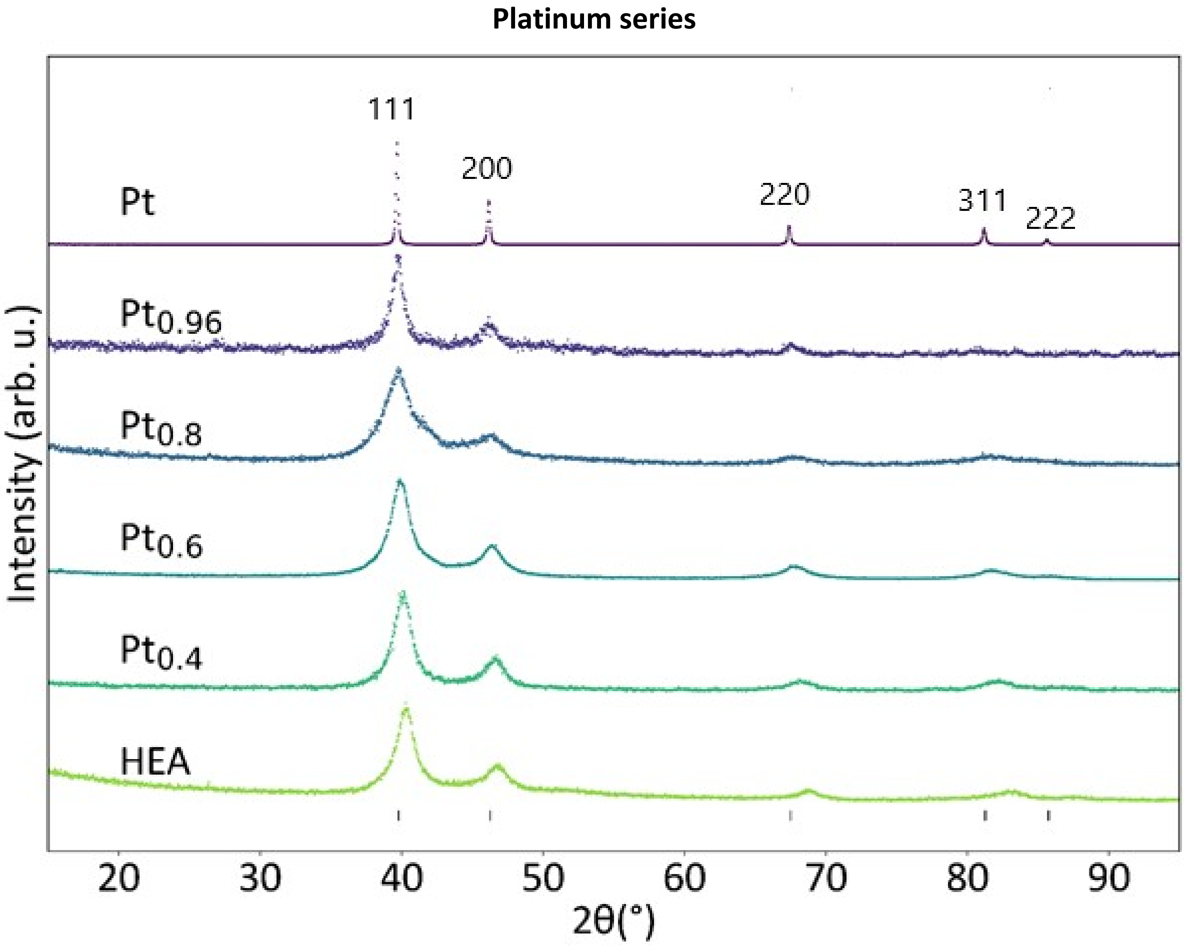

Figure S1. PXRD of $(IrPdRhRu)_{1-x}Pt_x$ series.

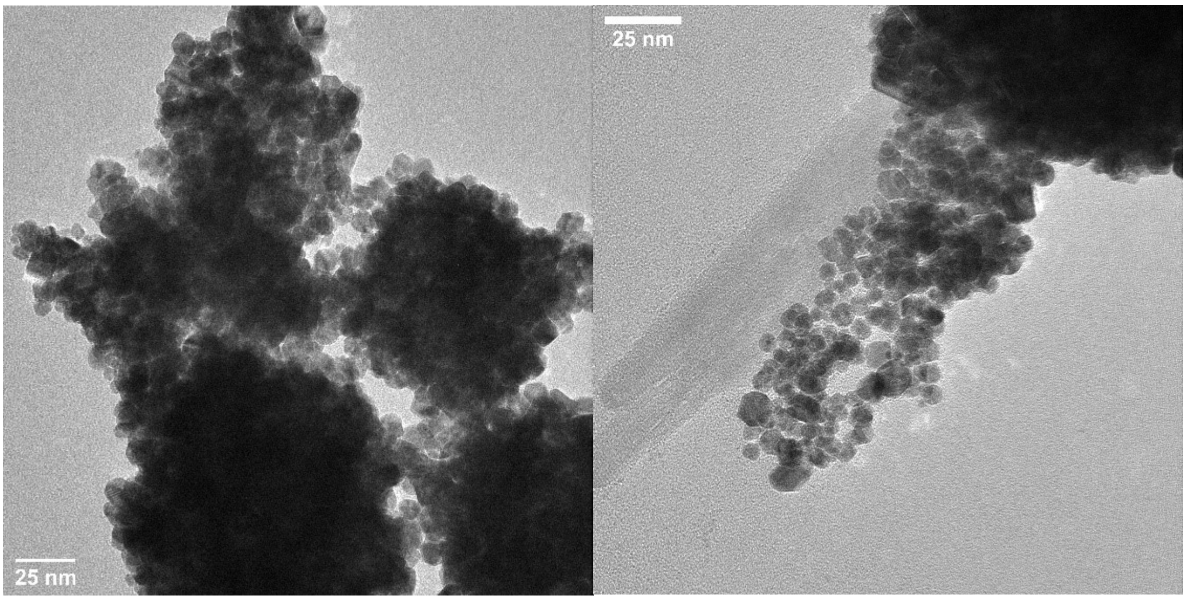

Figure S2. TEM images of $Pt_{0.4}$ (left) and $Pt_{0.6}$(right)

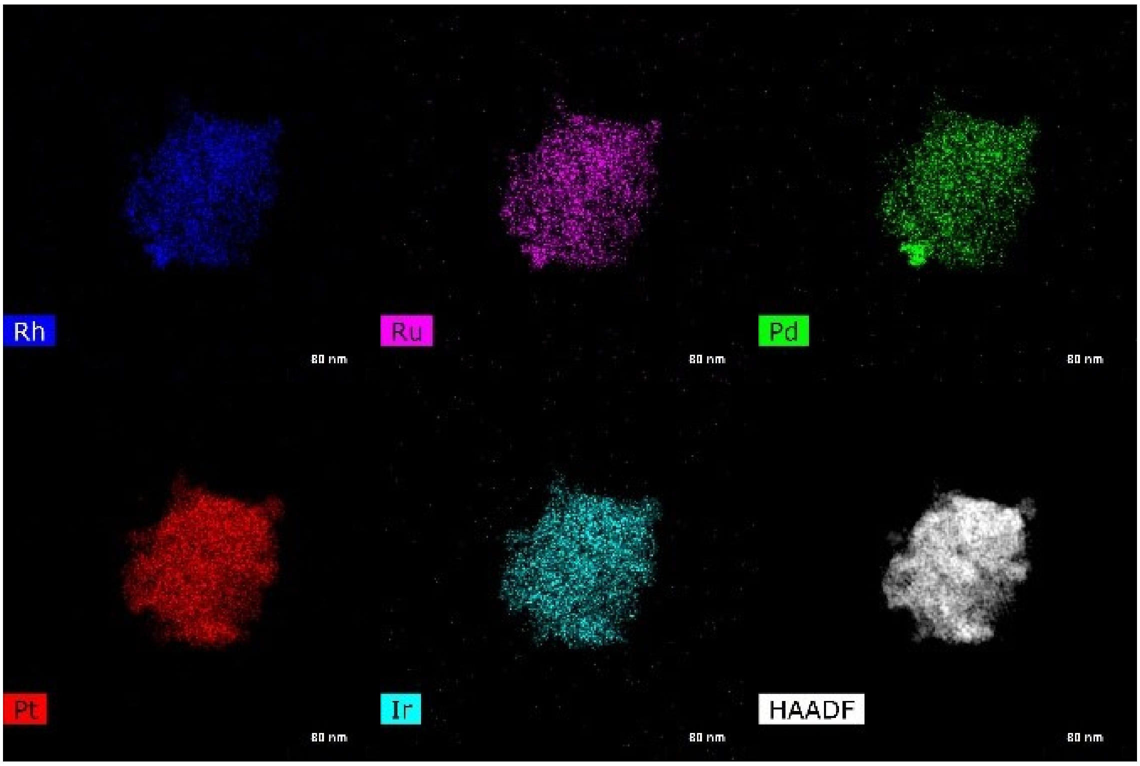

Figure S3. STEM-EDS images of $Pt_{0.8}$

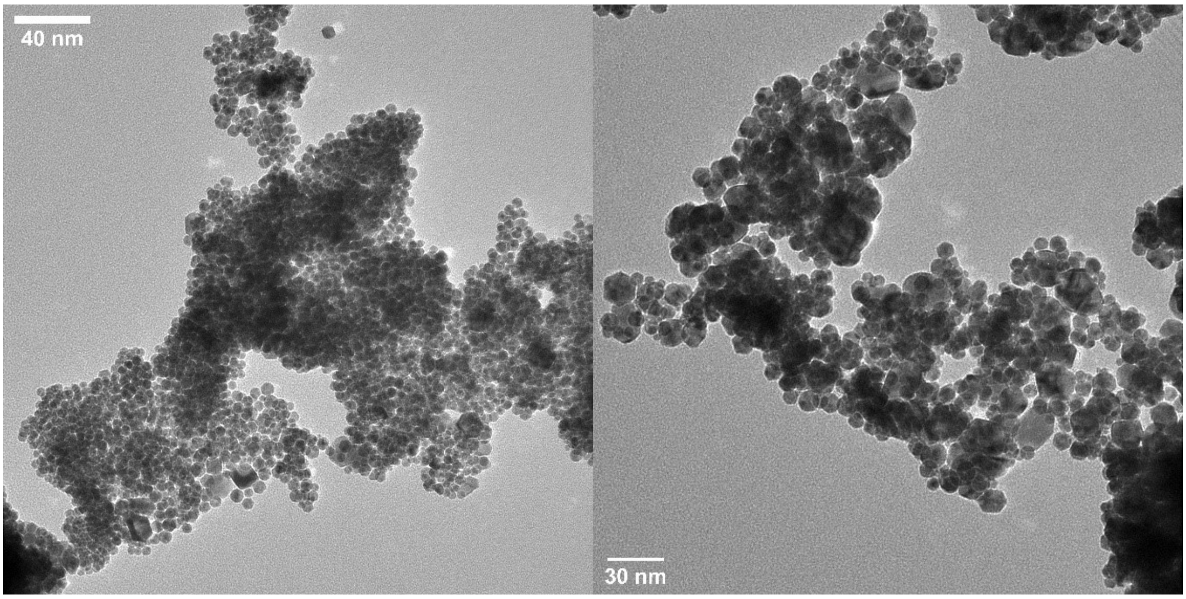

Figure S4. TEM images of $Pt_{0.8}$ (left) and $Pt_{0.96}$(right)

Rhodium series

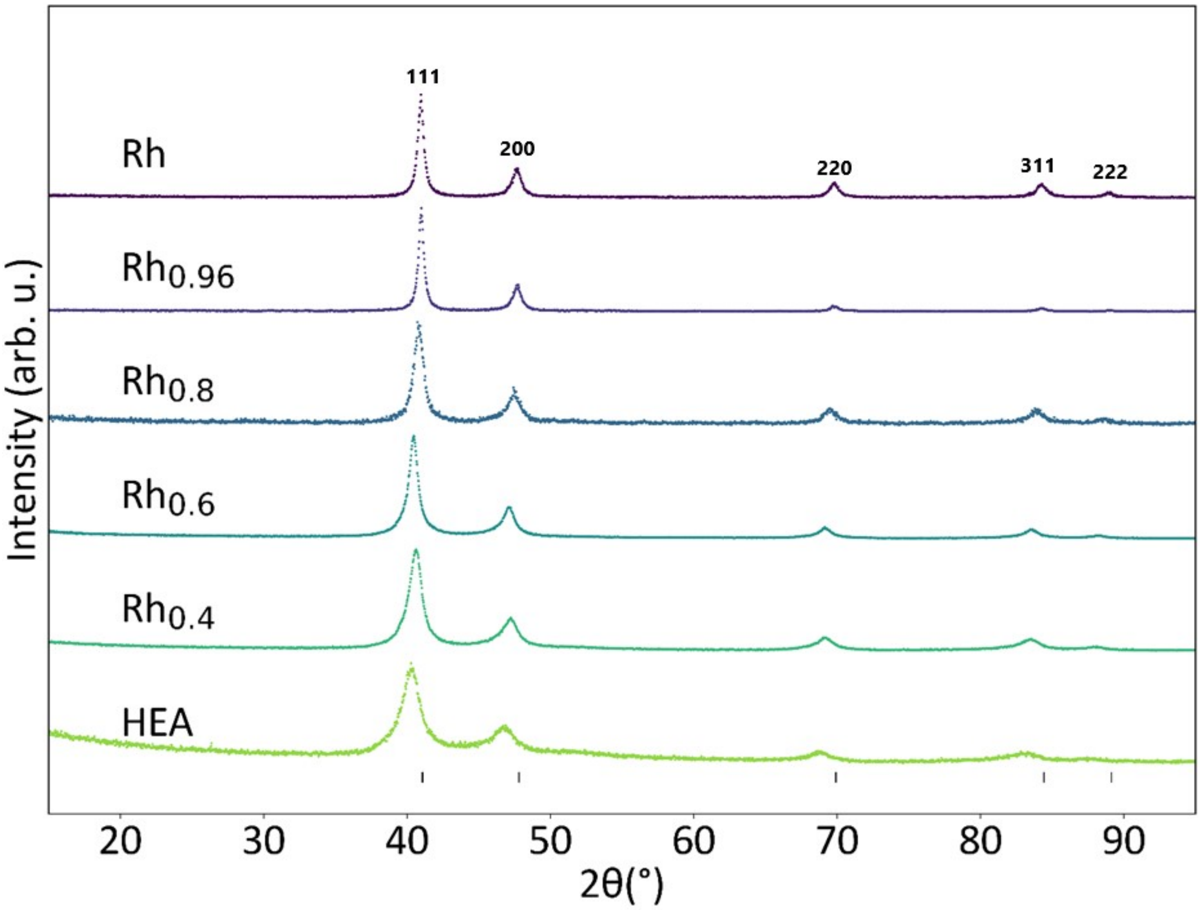

Figure S5. PXRD of $(PtIrPdRu)_{1-x}Rh_x$ series.

Palladium series

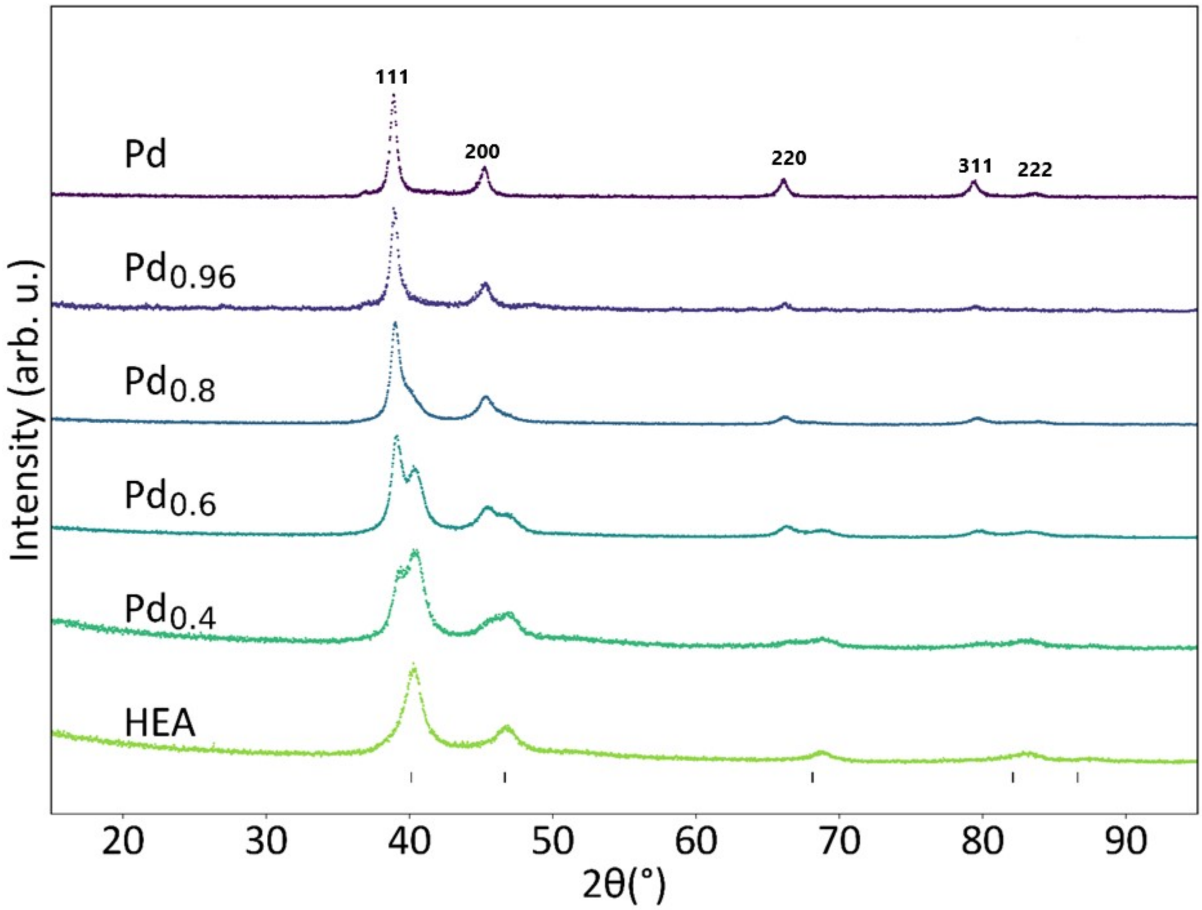

Figure S6. PXRD of $(PtIrRhRu)_{1-x}Pd_x$ series.

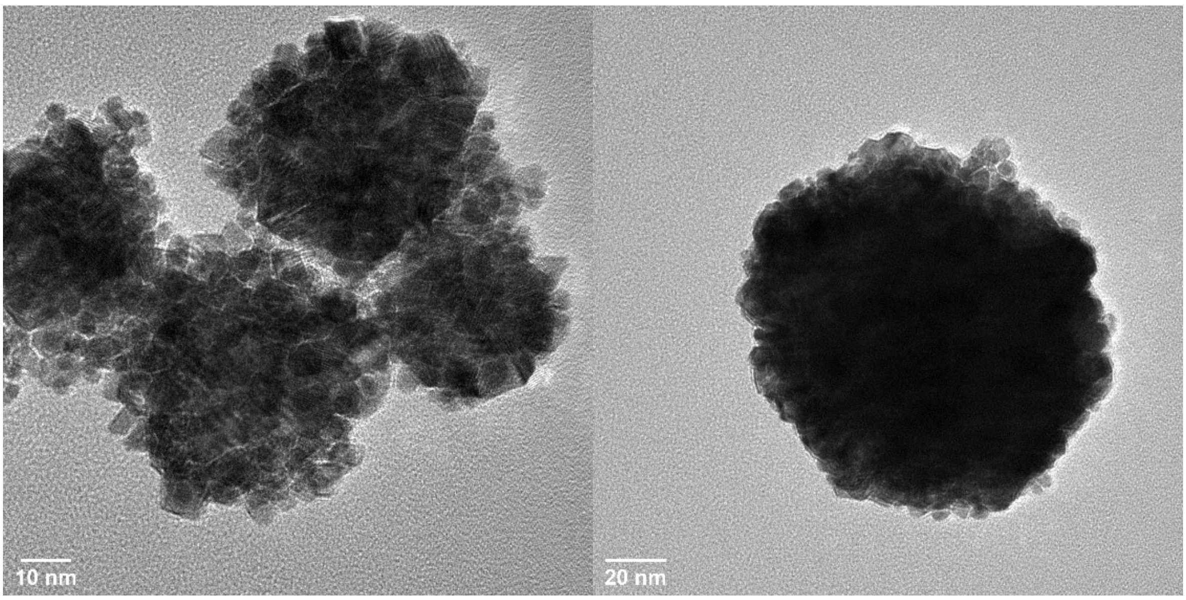

Figure S7. TEM images of $Pd_{0.4}$ (left) and $Pd_{0.6}$ (right)

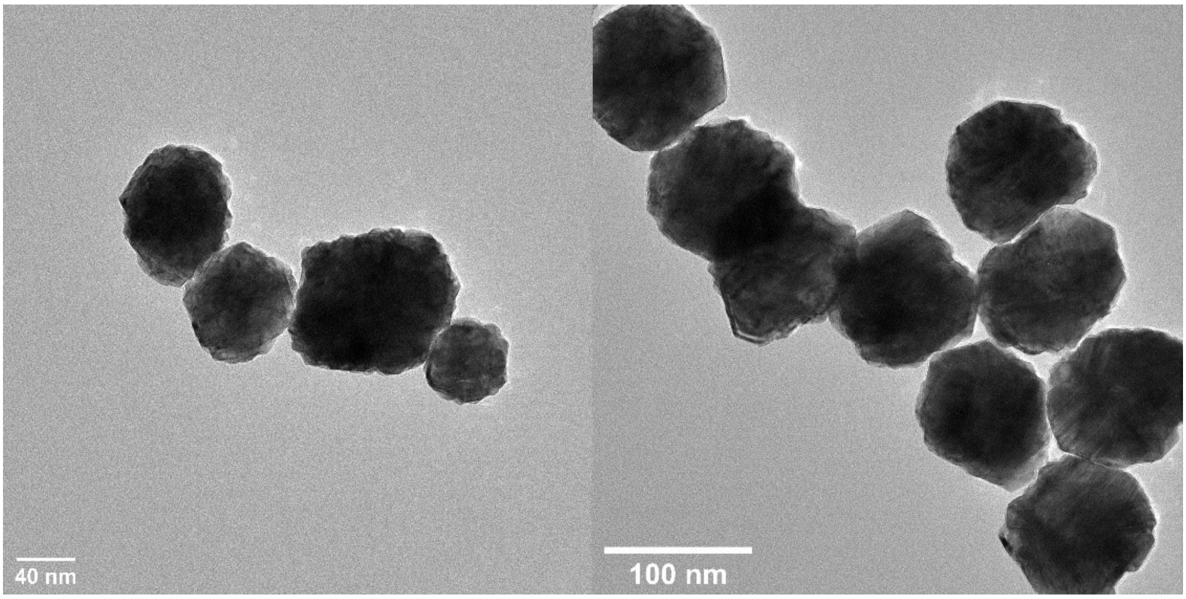

Figure S8. TEM images of $Pd_{0.8}$ (left) and $Pd_{0.96}$ (right)

Ruthenium series

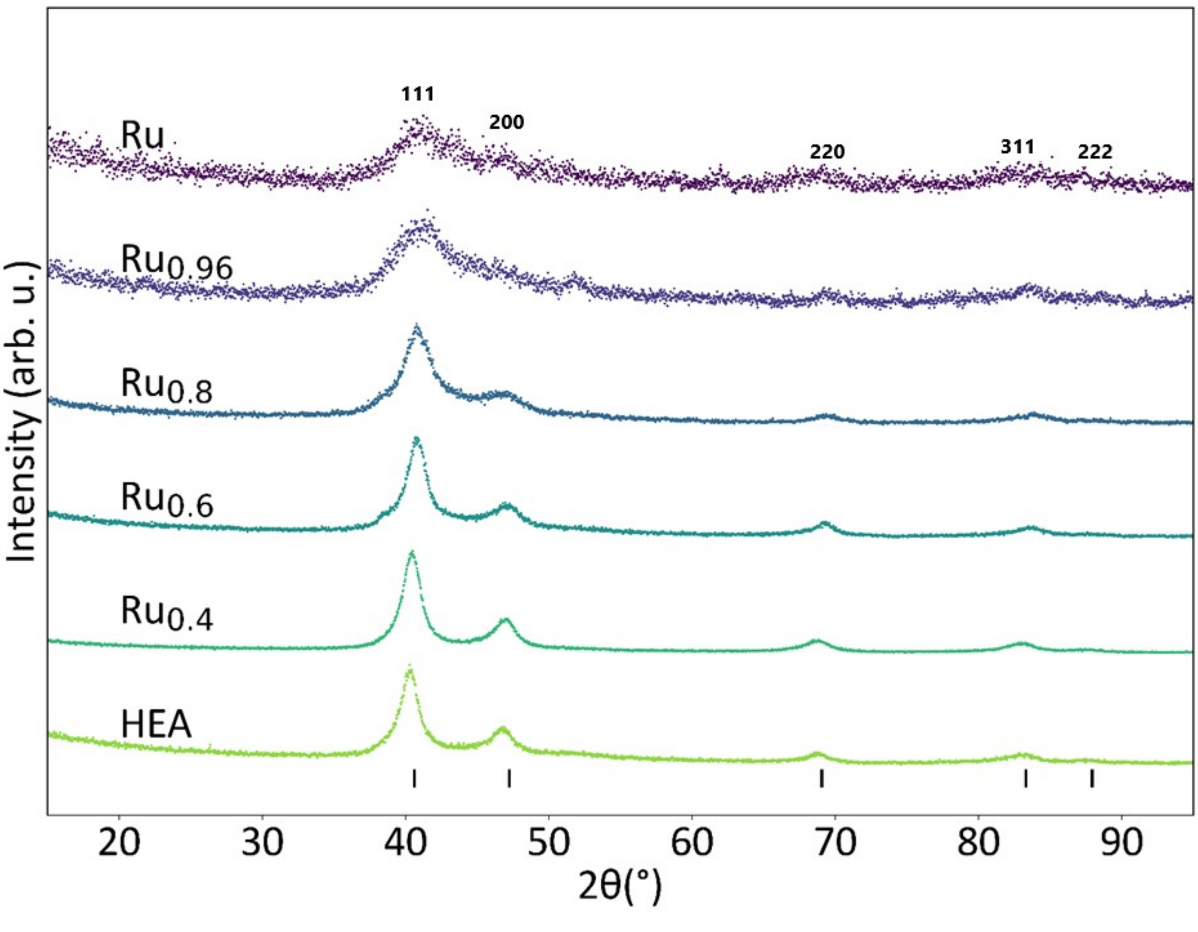

Figure S9. PXRD of $(PtIrPdRh)_{1-x}Ru_x$ series.

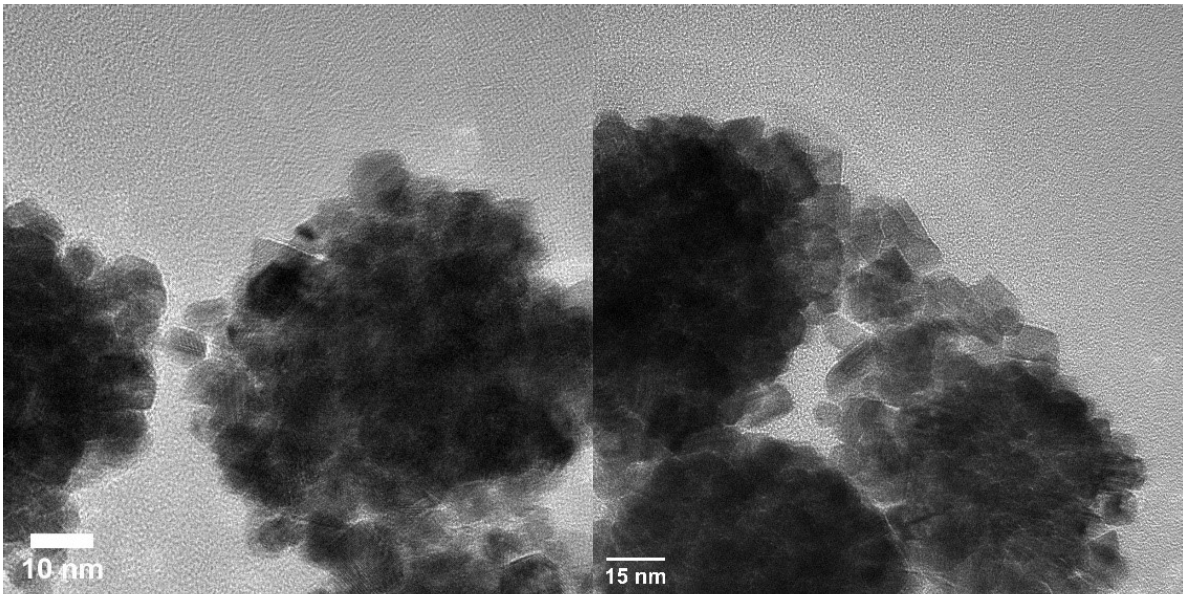

Figure S10. TEM images of $Ru_{0.4}$ (left) and $Ru_{0.6}$ (right)

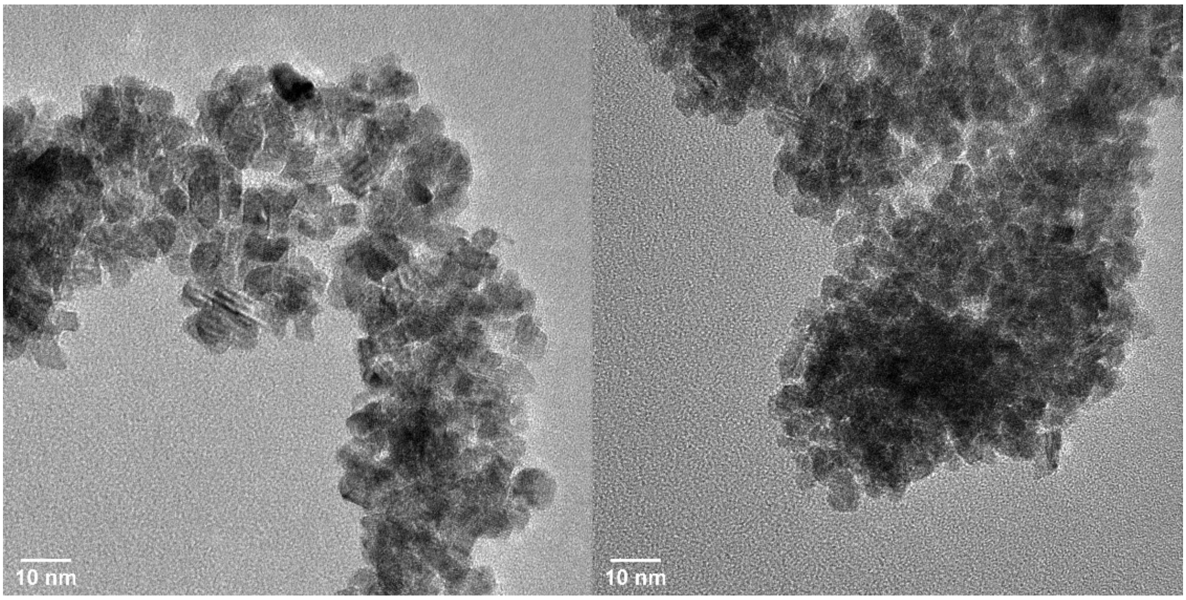

Figure S11. TEM images of $Ru_{0.8}$ (left) and $Ru_{0.96}$ (right)

Iridium series

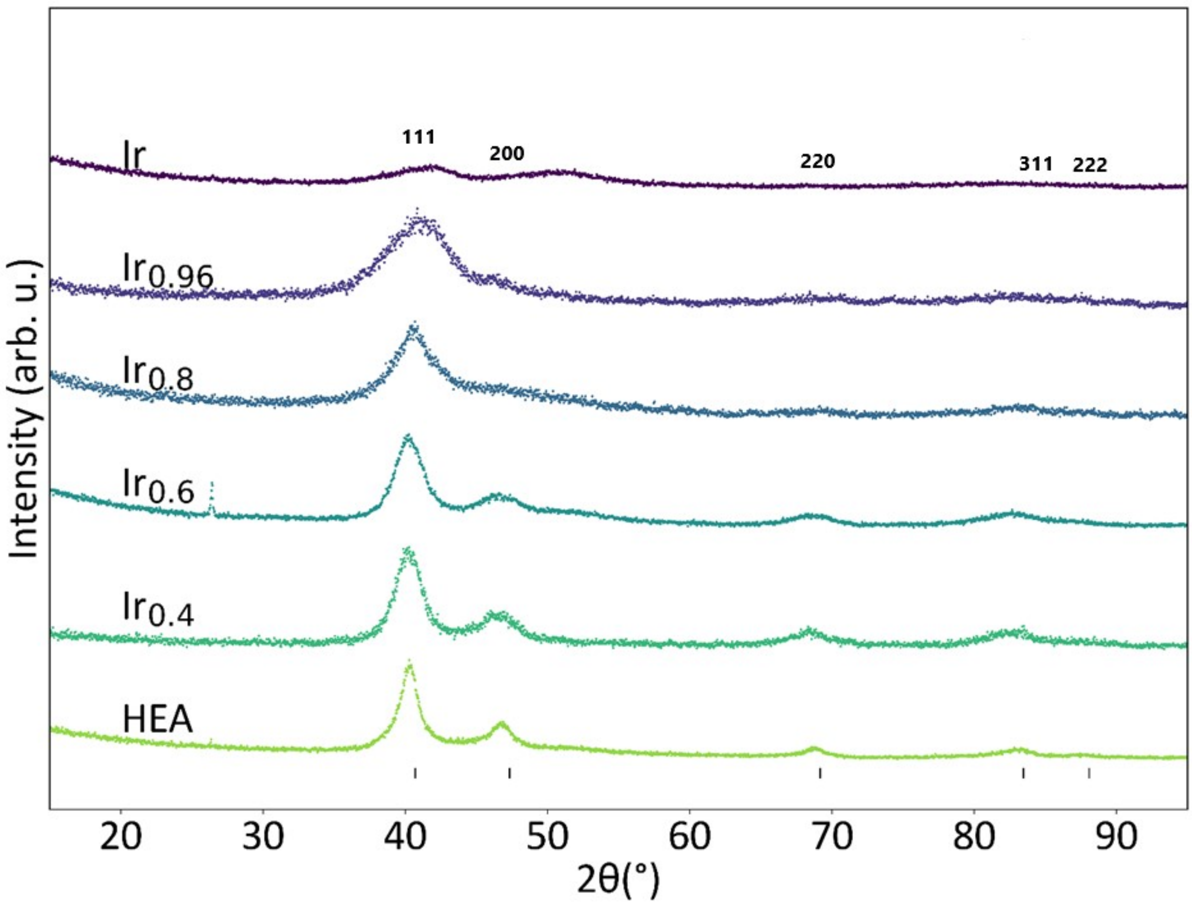

Figure S12. PXRD of $(PtPdRhRu)_{1-x}Ir_x$ series.

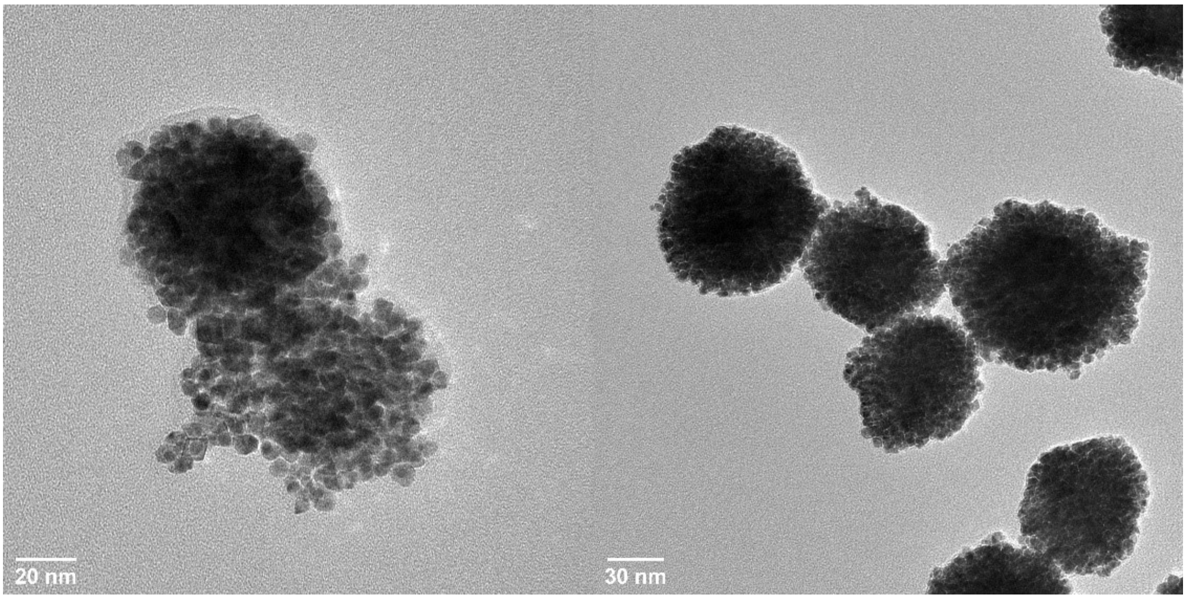

Figure S13. TEM images of $Ir_{0.4}$ (left) and $Ir_{0.6}$ (right)

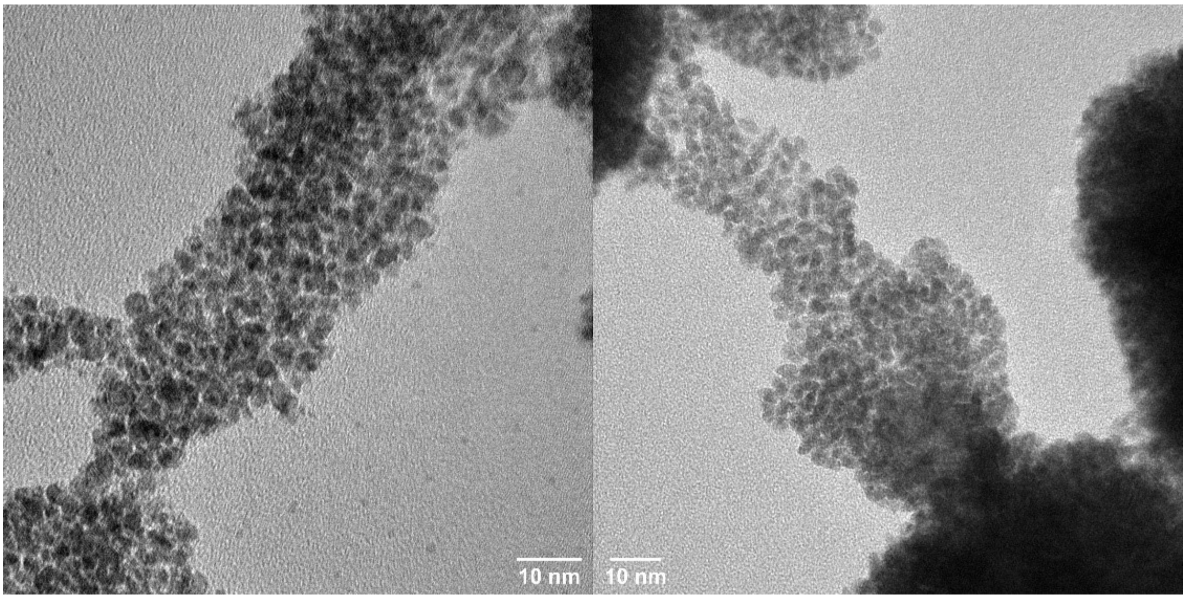

Figure S14. TEM images of $Ir_{0.8}$ (left) and $Ir_{0.96}$ (right)

Results of Le Bail fits

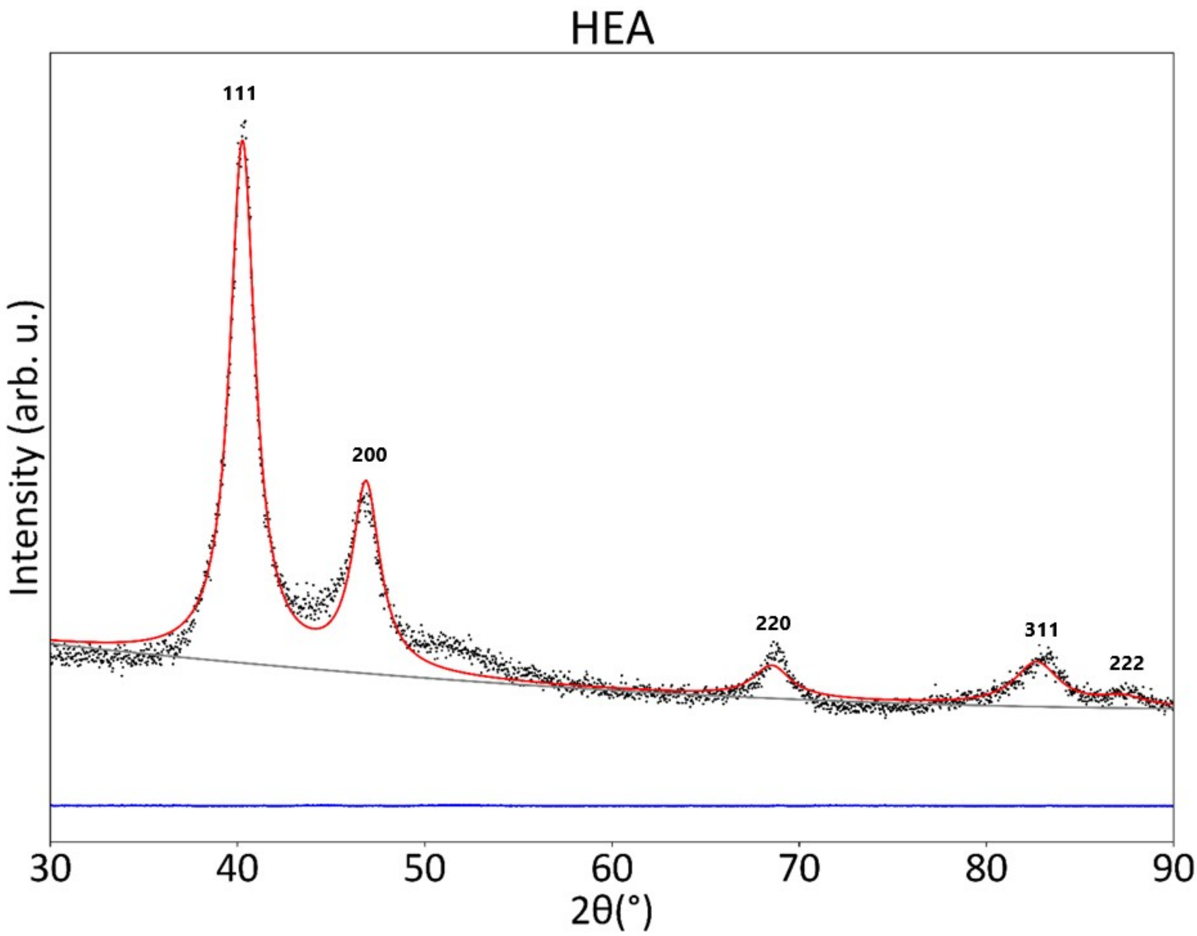

Figure S15. Le Bail Fit of the equimolar sample.

Tabel S1. Unit cell parameters obtained from Le bail fitting

Samples	0.4	0.6	0.8	0.96	1
Pt	3.892(1)	3.9086(8)	3.911(3)	3.923(4)	3.92675(4)
Rh	3.8421(5)	3.8357(5)	3.8228(5)	3.8109(4)	3.8085(2)
Ru	3.8626(1)	3.8316(4)	3.8231(6)	-	-
Ir	3.878(1)	3.869(3)	3.8430(9)	-	-
Pd small	3.862(3)	3.865(1)	3.903(2)	-	-
Pd Big	3.973(3)	3.989(1)	3.9962(9)	3.998(2)	3.9963(3)

Tabel S2. R-factors obtained from Le bail fitting

Sample\Parameter	R_wp	R_p	R_exp
Pt	5.38	12.95	0.4689
$Pt_{0.96}$	19.37	22.86	3.7532
$Pt_{0.8}$	10.52	11.17	0.7023
$Pt_{0.6}$	5.96	6.53	0.1727
$Pt_{0.4}$	8.79	11.00	1.0565
Rh	7.93	13.72	0.9087
$Rh_{0.96}$	6.57	14.15	0.7679
$Rh_{0.8}$	11.66	16.13	1.8912
$Rh_{0.6}$	7.30	9.93	0.1411
$Rh_{0.4}$	6.98	8.25	0.1472
Pd	11.62	19.17	1.2349
$Pd_{0.96}$	15.71	22.91	2.2699
$Pd_{0.8}$	7.44	10.70	0.3591
$Pd_{0.6}$	6.91	8.55	0.2444
$Pd_{0.4}$	9.49	10.06	0.5051
$Ru_{0.8}$	11.29	11.30	0.6647
$Ru_{0.6}$	11.60	11.60	0.4465
$Ru_{0.4}$	6.47	7.89	0.2658
$Ir_{0.8}$	12.57	11.84	1.0155
$Ir_{0.6}$	11.95	10.02	0.3204
$Ir_{0.4}$	13.51	15.30	2.1369
$HEA_{0.2}$	10.39	10.48	0.4165